Selective High-Resolution Electrodeposition on Semiconductor Defect Patterns

P. Schmuki[1,*] and L. E. Erickson[2]

[1]*Swiss Federal Institute of Technology (EPFL), Department of Materials Science, LC-DMX, CH-1015 Lausanne, Switzerland*
[2]*Institute for Microstructural Sciences, National Research Council of Canada (NRC), Ottawa, Ontario K1A 0R6, Canada*

(Received 27 June 2000)

We report a new principle and technique that allows one to electrodeposit material patterns of arbitrary shape down to the submicrometer scale. We demonstrate that an electrochemical metal deposition reaction can be initiated selectively at surface defects created in a p-type Si(100) substrate by Si^{++} focused ion beam bombardment. The key principle is that, for cathodic electrochemical polarization of p-type material in the dark, breakdown of the blocking Schottky barrier at the semiconductor/electrolyte interface occurs at significantly lower voltages at implanted locations than for an unimplanted surface. This difference in the threshold voltages is exploited to achieve selective electrochemical deposition.

PACS numbers: 68.55.Ln, 61.72.–y, 81.65.–b, 82.45.+z

Electrochemical deposition of metals and alloys onto metallic substrates plays an important role in many modern technologies. In the electronics industry, electrochemical and electroless deposition are widely used for applications, such as copper printed circuit boards, through-hole plating, multilayer read/write heads, and thin film magnetic recording media [1,2]. Surprisingly, there have been relatively few reports on the electroless [3–8], or electrochemical [9–20], deposition of metals onto semiconductors despite the technological importance of metal/semiconductor contacts for Schottky junctions and metallization. However, the recent success in replacing aluminum metallization by copper in silicon device technology (see, e.g., Refs. [21,22]) has led to a renewal of interest in electrochemical deposition of metals onto silicon as well as onto various barrier materials.

In order to create patterned metal structures, techniques based on classical lithography are employed. For high resolution patterning, most frequently e-beam or ion beam lithography are used (see, e.g., Ref. [23]). Recently, the development of the so-called LIGA (Lithographische Galvanische Abformtechnik) technique [24,25] that uses x-ray photoresist templates to produce high resolution "3D" electrodeposited structures has found considerable scientific interest. However, apart from the necessity to fabricate masks as demanded in these methods, the techniques imply that photoresists are provided that are resistant to the deposition or etching environment.

In contrast to masking approaches, far fewer attempts have been made to employ direct patterning processes. An interesting electrochemical deposition approach is based on native differences in the substrate reactivity. This is, for instance, the case for electrodeposition reactions on monotomic edges of terraces of a single crystal substrate (see, e.g., Refs. [26,27]). Ion implantation in Si is frequently used in the production process of integrated circuits, to dope near surface regions of the substrate (see, e.g., Refs. [28,29]). Apart from this primary doping effect, the high energy implantation process is accompanied by the generation of defects in the substrate surface and underlying lattice [30,31]. In a previous Letter, we reported how defects intentionally introduced in a surface by focused ion beam (FIB) bombardment can be used to selectively trigger an electrochemical etching reaction to form light emitting porous Si [32].

In the present Letter, we report the selective deposition of metals using the principle outlined in Fig. 1. A p-type semiconductor/electrolyte interface, when electrochemically biased, shows a similar electrical characteristic as a metal/semiconductor or p/n junction, i.e., a diode behavior with a current passing state when forward biased and a blocking state when reverse biased. In the blocking state a specific "barrier breakdown" potential U(Bd) exists that has been ascribed to Schottky barrier breakdown of the junction. At U(Bd), electrochemical reactions are not

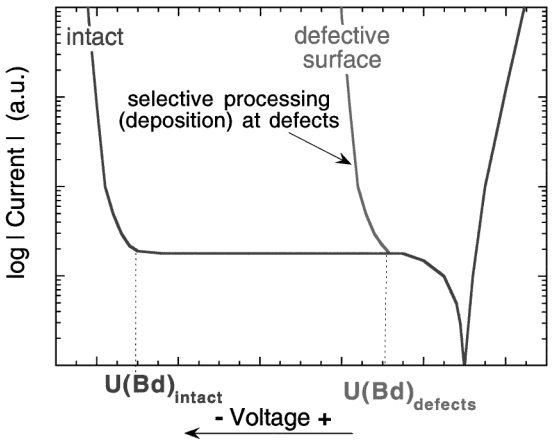

FIG. 1. Schematic current-voltage curve of a p-type semiconductor polarized in an electrolyte. The semiconductor/electrolyte interface shows a current blocking characteristic under cathodic bias up to the Schottky barrier breakdown potential U(Bd) (solid curve). At potentials cathodic to U(Bd), significant current flow is observed and electrochemical surface reactions take place. For a surface that has been damaged by ion implantation (dashed curve), the threshold potential $U(Bd)_{defects}$ is significantly lower. As a consequence, in the processing window between $U(Bd)_{intact}$ and $U(Bd)_{defects}$, electrochemical reactions are initiated selectively on the implanted regions.

hampered any longer by insufficient availability of charge carriers and thus can proceed at significant rates. The value of U(Bd) is strongly affected by surface defects, i.e., breakdown occurs for much lower applied bias voltages than for the intact surface, opening a window for selective processing between the two threshold voltages.

To create defined defect patterns with a high lateral resolution, Si^{++} ion patterns were implanted into phos phorus doped (1–10 Ω cm), p-type Si(100) wafers at room temperature with a 100 kV JEOL 104 UHV FIB system. Si^{++} was selected as the implanting species because chemical effects such as substrate doping are avoided. Moreover, Si^{++} is a sufficiently light element to minimize surface sputtering effects and to achieve mainly implantation and defect creation. Si^{++} ions from a Au-Si liquid metal ion source were selected (at 60 and 200 keV, respectively) using an $E \times B$ mass filter. The nominal beam width—controlled by an aperture—was 150 nm (defined as the full width at half maximum of an approximately Gaussian beam shape). By vector scanning the ion beam, different patterns (squares, lines, letters, dots) were implanted. Each pattern was implanted with dosages of 3×10^{13}, 10^{14}, 3×10^{14}, and 10^{15} ions/cm^2.

The number and distribution of defects created by the implantation can be estimated by calculations using TRIM code [30]. The calculation of the vacancy depth profile shows that creation of vacancies occurs immediately below the surface, and peaks at ≈50 nm below the surface for 50 keV implantation and at ≈250 nm below the surface for 200 keV implantation.

The implanted samples were then electrochemically treated under different conditions. Electrochemical polarization was carried out by voltage sweep experiments (polarization curves) where the voltage (electrochemical potential) was stepped by 10 mV every second in the cathodic direction. The potentials were measured and are reported versus the saturated calomel electrode (SCE). The electrochemical treatments were performed in the dark to avoid light induced carrier generation in the semiconductor sample. Electrodeposition of Au was carried out in an electrolyte consisting of $1M$ KCN + $0.01M$ $KAu(CN)_2$ or alternatively in $0.1M$ H_2SO_4 + $0.01M$ $CuSO_4$ to deposit copper.

In preliminary experiments, the threshold voltages for metal deposition for the defective surface, $U(Bd)_{defects}$, were determined as −1.3 V (SCE), for the alkaline Au containing electrolyte, and −0.5 V (SCE) for the acidic Cu electrolyte. For the intact p-type Si surface $U(Bd)_{intact}$ was in every case < -10 V (SCE).

Figure 2 shows examples of the surface morphology of locally implanted samples after an electrochemical treatment at potentials between $U(Bd)_{defects}$ and $U(Bd)_{intact}$. The letters and lines were written with the FIB and subsequently electrochemically "developed" from the latent implanted areas by Au electrodeposition. The scanning

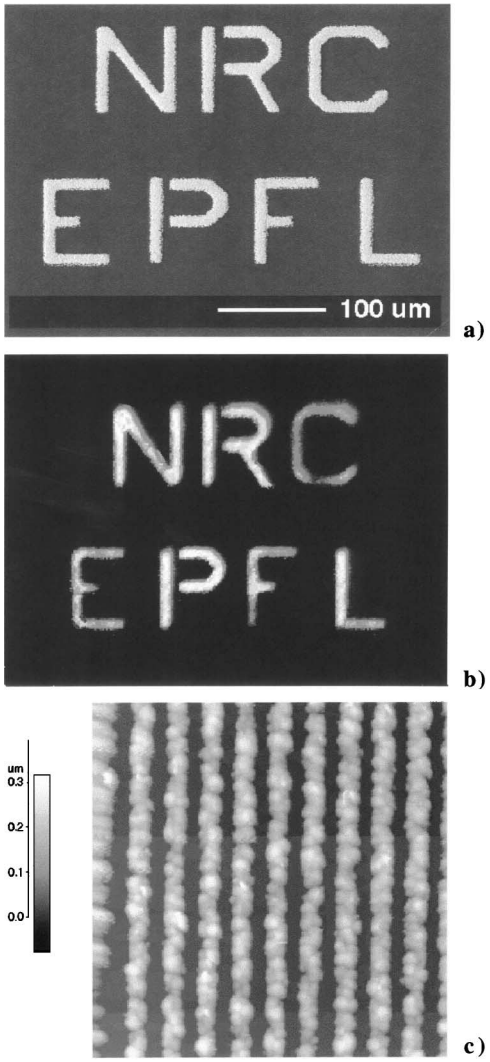

FIG. 2. Selective Au deposition on p-Si (100): (a) SEM image and (b) scanning AES image for Au of letters written with a Si^{++} ion dose of 10^{14} cm^{-2} followed by polarization from −900 to −5000 mV in a $1M$ KCN + $0.01M$ $KAu(CN)_2$ electrolyte (leading to Au deposition only on the implanted regions); (c) AFM topography image of Au lines electrodeposited selectively on single FIB implant lines (Si^{++} at a dose of 3×10^{14} cm^{-2}) under the same electrochemical conditions as in (a) and (b) (the AFM image size is 8×8 μm).

electron microscope (SEM) image in Fig. 2(a) shows selective deposition of gold on the implanted areas. The scanning Auger electron spectroscopy (AES) map for Au [Fig. 2(b)] for the deposit of Fig. 2(a) demonstrates that the deposition takes place with a very high selectivity. (Presence of Au is not detectable outside the implanted region.) A corresponding AES map for Si in the implanted letters indicates no detectable Si. Therefore, the deposit is coherent and no uncovered Si areas are present. The Au lines shown in the atomic force microscope image in Fig. 2(c) were deposited on single line FIB implants and show a width of 300–500 nm and a height of approximately 200 nm; i.e., selective and coherent

deposition can clearly be achieved with a submicrometer lateral resolution.

The morphology of the deposited features was found to depend strongly on the implant dose and the applied potential. For homogeneously implanted samples at different doses, a potential sweep from -0.9 V to -3 V results in complete Au coverage only for the highest investigated implant dose of 10^{15} ions/cm^2. At the lower doses (3×10^{14}, 10^{14} ions/cm^2), deposition results in isolated globular structures. The surface density of these globular deposits, corresponding to successful Au nucleation/growth sites, decreases with a lower implant dose. For a dose of 3×10^{13} ions/cm^2 no Au deposition could be detected. This finding shows that nucleation and growth of Au clusters on the Si surface is strongly interlinked with the defect density introduced by the ion bombardment.

For potential sweep experiments from -0.9 to -5 V, a dose of 10^{14} cm^{-2} leads to a complete coherent coverage of the implanted region (such as in Fig. 2). This indicates that, for each polarization potential, a different critical defect density has to be established to achieve a coherent coverage of the implanted surface. Such coherent features obtained by polarization to -3 or -5 V typically have a height of 50–200 nm (obtained from atomic force topography mapping as in Fig. 2(c).

In general, nucleation and growth of a metal deposited on a foreign substrate can either be of a 2D film type or a 3D island formation or intermediate cases [33]. For metal deposition onto semiconductors, the interaction forces between adsorbed metal atom (adatom) and the semiconductor surfaces are usually relatively weak (compared with metal-metal interactions). Thus, often a 3D island growth is predominant [33] as in our case. As a result, nucleation and growth will follow a Volmer-Weber–type kinetics [34]. This implies that the number of successfully triggered nucleation sites is strongly potential dependent. In other words, at lower applied potentials, where only a few nucleation sites are triggered, the clusters would have to grow extremely large to reach coalescence to a continuous film.

Another factor that strongly affects the deposition process is the energy used for ion implantation. Some experiments were carried out with Si(100) samples carrying defect patterns created by Si^{++} implantation at 200 keV. Even for implant doses of 10^{15} cm^{-2} polarization in $1M$ KCN + $0.01M$ $KAu(CN)_2$ to -5 V does not reveal any deposition. This can be explained by considering the implant/defect profiles for 50 and 200 keV. According to TRIM calculation for 200 keV implantation, the damage profile peaks at $\approx$250 nm below the surface; i.e., after implantation a relatively thick outermost layer of the substrate is present that is less defective than an underlying "maximum damage" layer. Such a relatively undamaged surface layer is frequently observed after high energy ion implantation (see, e.g., Refs. [35–37]). This top layer can be removed by a uniform chemical etch. For samples implanted at 200 keV, after etching the top 150–200 nm of the Si sample [samples were dipped for 10 s in a chemical etching solution (300 ml HNO_3 65% + 200 ml CH_3 COOH 100% + 20 ml HF 48%) with a nominal Si etch rate of 1 μm/min at RT], selective electrochemical deposition can be achieved easily.

An example with such a preetched Si sample is shown in Fig. 3 for the selective deposition of Cu patterns on the Si(100) surface. In this case, the letters were written with single Si^{++} FIB lines with a nominal width of 200 nm at 200 keV with a dose of 3×10^{14} cm^{-2}. The surface then was uniformly preetched and, subsequently, Cu deposition was carried out by polarizing the samples from -0.5 to -2 V at -10 mV/s in $0.1M$ H_2SO_4 + $0.01M$ $CuSO_4$. The width of the deposited Cu letters results as approximately 200–300 nm. These findings clearly indicate that the etching pretreatment exposes higher defect concentration and thus facilitates deposition and suggests that metal nucleation and growth is either linked to a critical defect density or that for Schottky barrier breakdown at sufficiently low potentials a critical defect density is necessary. Additionally, the result in Fig. 3 shows that the resolution of the deposition can be in the range of the nominal implant width. In other words, under ideal electrochemical conditions, the lower lateral resolution limit of the deposition process mainly depends on the diameter of the writing ion beam.

In summary, we have shown how a semiconductor electrode can be "activated" for a subsequent selective electrochemical reaction by intentionally creating defined surface defects at desired surface sites, and more specifically how to produce laterally confined metal structures on Si by a direct writing process. At present, the best resolution obtained lies in the 100 nm range but could be optimized to even smaller dimensions (using a smaller diameter of the

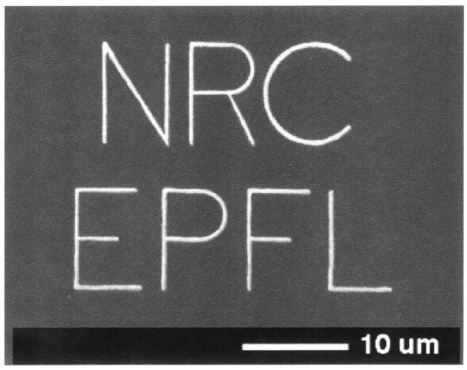

FIG. 3. SEM micrograph of selectively electrodeposited Cu letters on p-type Si(100). The latent letter patterns were FIB written with Si^{++} ions at 200 keV and a dose of 3×10^{14} cm^{-2}. Then the maximum damage zone was exposed using a uniform chemical Si etch and Cu was deposited by polarizing the sample in $0.1M$ H_2SO_4 + $0.01M$ $CuSO_4$ from -0.5 to -2 V SCE. The letters were implanted with a nominal ion beam width of 200 nm; the width of the deposited Cu letters results as 200–300 nm.

writing ion beam). The results, at present, suggest that this principle is not restricted to the example investigated within this work (selective Au or Cu deposition on p-type Si) but generally can be applied to any electrodeposition on semiconductor reaction. Since, other than metals, a wide range of materials can be electrodeposited (e.g., semiconductors, polymers, or ceramics), the process opens up wide possibilities for nanostructuring of materials. As the patterning of semiconductor surfaces with a variety of materials is of a high scientific and technological importance, e.g., for modern device development, the process provides a new tool for selectively adding new functionality to a semiconductor surface.

We would like to thank G. Champion, G. I. Sproule, T. Djenizian, and L. Santinacci for their meticulous help with the experiments and the Swiss National Science Foundation and COST523 for the financial support of this project.

*Present address: University of Erlangen-Nuremberg, Department of Materials Science, LKO, D-91058 Erlangen, Germany.

[1] L. T. Romankiw and T. A. Palumbo, in *Electrodeposition Technology, Theory and Practice,* edited by L. T. Romankiw and D. R. Turner (Electrochemical Society, Pennington, NJ, 1987), Vol. **PV/87-17**, p. 764.
[2] P. S. Searson and T. P. Moffat, Crit. Rev. Surf. Chem. **3**, 171 (1994).
[3] H. Morinaga, M. Suyama, and T. Ohmi, J. Electrochem. Soc. **141**, 2834 (1994).
[4] G. J. Norga, M. Platero, K. A. Black, A. J. Reddy, J. Michel, and L. C. Kimerlin, J. Electrochem. Soc. **144**, 2801 (1997).
[5] C.-A. Chang, J. Appl. Phys. **67**, 566 (1989).
[6] J. Li and Y. Sacham-Diamand, J. Electrochem. Soc. **137**, L37 (1992).
[7] C. H. Ting and M. Paunovic, J. Electrochem. Soc. **136**, 456 (1989).
[8] S. Furukawa and M. Mehregany, Sens. Actuators A **56**, 261 (1996).
[9] P. Gorostiza, J. Servat, R. Diaz, F. Sanz, and J. R. Morante, MRS Proc. **451**, 275 (1997).
[10] P. M. Hoffman, J. G. Long, P. J. Moran, and P. Searson, ECS Meeting Abstracts **98-1**, 246 (1998).
[11] G. Oskam, D. vanHeerden, and P. C. Searson, Appl. Phys. Lett. **73**, 3241 (1998).
[12] L. A. D'Asaro, S. Nakahara, and Y. Okinaka, J. Electrochem. Soc. **127**, 1935 (1989).
[13] P. Bindra, H. Gerischer, and D. M. Kolb, J. Electrochem. Soc. **124**, 1012 (1977).
[14] R. Reineke and R. Memming, Surf. Sci. **192**, 66 (1987).
[15] P. Allongue and E. Souteyrand, J. Vac. Sci. Technol. B **5**, 1644 (1987).
[16] G. Oskam, L. Bart, D. Vanmaekelbergh, and J. J. Kelly, J. Appl. Phys. **74**, 3238 (1993).
[17] G. Oskam, D. Vanmaekelbergh, and J. J. Kelly, Electrochim. Acta **38**, 1115 (1993).
[18] P. Allongue and E. Souteyrand, J. Electroanal. Chem. **362**, 79 (1993).
[19] G. Scherb and D. M. Kolb, J. Electroanal. Chem. **396**, 151 (1995).
[20] P. M. Vereecken, K. Strubbe, and W. P. Gomes, J. Electroanal. Chem. **433**, 19 (1997).
[21] P. C. Andricanos, C. Uzoh, J. O. Dukovic, J. Horkans, and H. Deligianni, IBM J. Res. Dev. **42**, 567 (1998).
[22] P. C. Andricanos, Electrochem. Soc. Interface **8**, 32 (1999).
[23] *Electron-beam, X-ray, and Ion-beam Submicrometer Lithographies for Manufacturing,* edited by M. Peckerar, SPIE Proceedings (SPIE-International Society for Optical Engineering, Bellingham, WA, 1991), p. 1465; *ibid.* (1992), p. 1671; *ibid.,* edited by D. O. Patterson (1993), p. 1924; *ibid.* (1994), p. 2194; *ibid.,* edited by J. M. Warlaumont (1995), p. 2437; *ibid.,* edited by D. E. Seeger (1996), p. 2723.
[24] E. Spiller, R. Feder, J. Topalian, E. Castellani, L. Romankiw, and M. Heritage, Solid State Technol. (1976).
[25] W. E. Becker, W. Ehrfeld, D. Munchmeyer, H. Betz, A. Heuberger, S. Pongratz, W. Glashauser, H. J. Michel, and V. R. Siemens, Naturwissenschaften **69**, 520 (1982).
[26] K. Uosaki and H. Kita, J. Electroanal. Chem. **239**, 301 (1989).
[27] U. Schmidt, S. Vinzelberg, and G. Staikov, Surf. Sci. **348**, 261 (1996).
[28] S. M. Sze, *Physics of Semiconductor Devices* (Wiley, New York, 1981).
[29] H. G. Robinson, C. C. Lee, T. E. Haynes, E. L. Allen, M. D. Deal, and K. D. Jones, Mater. Res. Soc. Symp. Proc. **354**, 337 (1995).
[30] J. F. Ziegler, J. P. Biersack, and U. Littmark, *The Stopping and Range of Ions in Solids* (Pergamon, New York, 1985).
[31] P. Schmuki, L. E. Erickson, G. Champion, B. F. Mason, J. W. Fraser, and C. Moessner, Appl. Phys. Lett. **70**, 1307 (1997).
[32] P. Schmuki, L. E. Erickson, and D. J. Lockwood, Phys. Rev. Lett. **80**, 4060 (1998).
[33] E. Budewski, G. Staikov, and W. Lorenz, *Electrochemical Phase Formation and Growth* (VCH, Weinheim, 1996).
[34] M. Volmer and A. Weber, Z. Phys. Chem. **119**, 277 (1927).
[35] P. Schmuki, L. E. Erickson, D. J. Lockwood, B. F. Mason, J. W. Fraser, G. Champion, and H. J. Labbé, J. Electrochem. Soc. **146**, 735 (1999).
[36] R. J. Culbertson, D. W. Holland, K. J. Jones, and K. Maex, *Materials Synthesis and Processing Using Ion Beams* (Materials Research Society, Pittsburgh, 1994).
[37] L. E. Erickson, H. G. Champion, J. W. Fraser, R. Hussey, P. Schmuki, and C. Porco, J. Vac. Sci. Technol. B **15**, 2358 (1997).